Crystalline Morphology at the Interface between Polyethylene-Grafted Glass and Polyethylene

Jannick Duchet,[1] Jean-François Gérard,[1] Jean-Paul Chapel,[2] Bernard Chabert,[2] Josee Brisson[3]

[1]Laboratoire des Matériaux Macromoléculaires (LMM), UMR CNRS 5627, Institut National des Sciences Appliquées de Lyon (INSA), Bât. 403, 20 Avenue A. Einstein, 69621 Villeurbanne Cedex, France
[2]Laboratoire d'Etudes des Matériaux Plastiques et des Biomatériaux (LEMPB), UMR CNRS 5627, Université Claude Bernard Lyon I, Bât. 303, 43 Boulevard du 11 Novembre 1918, 69622 Villeurbanne Cedex, France
[3]Département de Chimie, Centre de Recherche en Sciences et Ingénierie des Macromolécules, Université Laval, Pavillon Alexandre, Vachon, Bureau 2220, Québec (Québec) Canada G1K 7P4

ABSTRACT: Adhesion measurements performed on a polyethylene (PE)-grafted-glass interface showed that the structure of the PE free chains (matrix) was an important parameter. The fracture energy was higher for interfaces prepared from a linear matrix, such as high-density polyethylene (HDPE), than for those from a branched PE [low-density polyethylene (LDPE)]. Therefore, the microstructure of the grafted PE/PE matrix interface or interphase was investigated as a function of the molar masses of the connectors and the structure (linear or branched) of the free PE matrix chains. As the grafted chains were linear, a cocrystalline structure with free chains of the HDPE matrix was generated. PE connecting chains led to a low capacity for cocrystallization with LDPE. Cocrystallization was studied with blends based on functionalized PE chains and PE matrices. These blends were assumed to be miscible, as substantiated by a single differential scanning calorimetry (DSC) peak. The DSC analyses were confirmed by wide-angle X-ray scattering, which revealed a crystalline orientation of the chains in the interphase, that is, in the vicinity of the glass surface. © 2002 Wiley Periodicals, Inc. J Appl Polym Sci 87: 214–229, 2003

Key words: crystallization; adhesion; polyethylene (PE)

INTRODUCTION

The fiber/matrix interface of composite materials is widely regarded as an important component for determining their mechanical behavior. Especially when the processing of semicrystalline thermoplastic materials is considered, changes in the matrix morphology in the vicinity of the fiber surface need to be taken into account. These microstructural changes may affect the fiber/matrix adhesion and interphase parameters as well. It is not clear yet how different morphological structures induced by processing in thermoplastic composites are involved with respect to the interfacial fracture energy (*G*) and the related failure mechanisms of the interface.

A new route was developed for modifying the glass/semicrystalline polymer interface by the grafting of connecting polymer chains having the same chemical nature as the matrix.[1,2] According to the compatibility between the tethered chains and the polymer used as the matrix, the tethered chains can interdiffuse into free polymer chain media. The enhancement of the interfacial adhesion is achieved by segmental interactions and by the creation of entanglements. Much of the fundamental work in this area has been devoted to the reinforcement of interfaces between glassy polymers with diblock copolymers.[3–6] Recently, this method was used for improving the adhesion between two semicrystalline polymers, polypropylene (PP) and polyamide 6,[7,8] by the in situ formation of a block copolymer at the interface. It was demonstrated that if the fracture mechanisms were similar to those observed at the interface between glassy polymers, the local crystalline organization of the chains governed the dissipation efficiency and the fracture toughness of the interface. A crystallographic analysis on the PP side of the interface showed a correlation between the presence of the PP *β* phase at the interface and a high value of the fracture toughness. The authors attributed this effect to the presence of the *β* phase of PP at the interface and to the subsequent formation of a much larger plastic zone. This result is the first evidence of the influence of the crystallinity of a semicrystalline polymer on its adhesive properties. Adhesion is a function of the bulk properties of both components and is a result of the crystallinity. Other works have focused on adhesion between semicrystalline polymers[9,10] and have shown that the formation of a linkage via cocrystallization between the grafted connectors and the matrix strongly improves adhesion in a composite. The cocrystallization

Correspondence to: J. Duchet.

TABLE I
Molar Masses of Connecting Chains and of PE Matrices

	M_n (g mol^{-1})	M_w (g mol^{-1})	IP[a]
PE1200-CI	1,194	5,230	4.4
PE3700-CI	3,710	16,000	4.3
EH32500-CI	32,500	65,000	2.0
HDPE	13,050	213,100	16.0
LDPE	19,350	106,700	5.5

[a] IP = index of polydispensity

is all the more favored, so connectors are long enough and regular with a low grafting ratio.[11] Moreover, the morphology of the interphase strongly depends on the processing conditions of the composite.[12]

In a previous article,[13] we reported that the adhesion developed at the polyethylene (PE)/glass interface was improved by PE chains grafted onto the glass surface. For both high-density polyethylene (HDPE)/glass and low-density polyethylene (LDPE)/glass interfaces, G was found to increase with the length of the connecting chains. However, the adhesion level was straightforwardly different as a function of the type of matrix.

The aim of this work was to correlate the fracture properties of considered interfaces with the molecular

structure in the interphase. By means of analysis techniques such as differential scanning calorimetry (DSC) and wide-angle X-ray scattering (WAXS), we were able to characterize for blends the miscibility on a molecular scale and the crystalline organization at the interface between grafted glass and PEs.
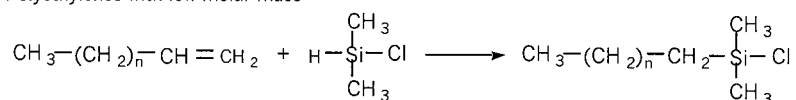
EXPERIMENTAL

Materials

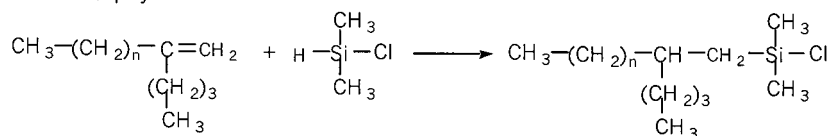**Polymer connectors: chlorosilane-functionalized PEs**

The PEs before functionalization were synthesized by polymerization with a metallocene catalyst in heptane. Two types of polymers were prepared: linear PEs (PE1200 and PE3700) and a copolymer based on ethylene and hexene (EH32500). The hexene-1 comonomer was used, with a 6.6% molar ratio, to reduce the regularity and, therefore, crystallinity of the resulting polymer. This synthesis is described in detail elsewhere.[14]

These polymers were silane-terminated by hydrosilylation at 90°C with a Speier hexachloroplatinic acid catalyst in xylene with chlorodimethylsilane (used as received from ABCR Products, Lauterbourg, France). The hydrosilylation can be described as follows:

Linear Polyethylenes with low molar mass

$$CH_3-(CH_2)_n-CH=CH_2 \;+\; H-\underset{CH_3}{\overset{CH_3}{Si}}-Cl \;\longrightarrow\; CH_3-(CH_2)_n-CH_2-\underset{CH_3}{\overset{CH_3}{Si}}-Cl$$

Ethylene-hexene Copolymer

$$CH_3-(CH_2)_n-\underset{(CH_2)_3}{\overset{}{C}}=CH_2 \;+\; H-\underset{CH_3}{\overset{CH_3}{Si}}-Cl \;\longrightarrow\; CH_3-(CH_2)_n-\underset{(CH_2)_3}{\overset{}{CH}}-CH_2-\underset{CH_3}{\overset{CH_3}{Si}}-Cl$$
$$\overset{}{\underset{CH_3}{}} \qquad\qquad\qquad\qquad \overset{}{\underset{CH_3}{}}$$

The disappearance of the double bonds (—CH=CH2) and the appearance of the silane functions were checked by Fourier transform infrared spectroscopy.[14]

PE matrices

HDPE and LDPE (FINA Chemicals, Lacq, France) were used as matrices for processing the PE/glass interface. PE films were prepared under a hot press at 180°C for 1 min and were cooled to room temperature (5°C min^{-1}).

The molar masses were measured by size exclusion chromatography and are reported in Table I.

PE–glass interface

The double-cantilever beam test used in the PE/glass experiments was performed with a specimen pre-

pared from two floating glass slides and a pure 200-μm-thick PE (HDPE or LDPE) film (Fig. 1). Silane-terminated PEs were grafted onto floating glass slides (50 × 15 × 2 mm^3). These were cleaned with a pirahna solution (70 vol % H$_2$SO$_4$ and 30 vol % H$_2$O$_2$) at 120°C, rinsed in deionized water, and further dried in nitro-
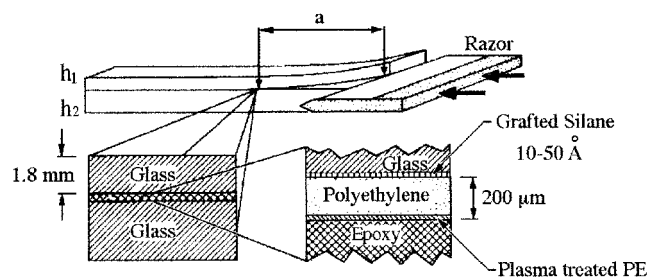

Figure 1 ADCB specimens (for more details, see ref. 13).

gen. On one side of the glass slide, the connecting chains were grafted by a solvent method in xylene under an argon atmosphere, as described elsewhere.[14] The dimers resulting from the self-condensation of two silane-terminated PE chains and/or physisorbed molecules were removed by extended Soxhlet extractions with xylene. The measured thickness of the dried grafted monolayers was 40–55 Å.[14] The grafted glass was joined to the PE film. In fact, to stiffen the PE film and to reduce the dissipative phenomena during the fracture test, a second glass slide was required on the other side of the PE film with an epoxy resin (Fig. 1). To obtain a sufficient level of PE–epoxy adhesion, the PE surface was subjected to an oxygen plasma with a postdischarge. The epoxy adhesive was then cured for 3 h at 50°C under 6 kPa.

The PE/glass interfaces were prepared at the melting temperature (T_m) of the corresponding PE for 3 h to ensure the interdiffusion of grafted chains in the molten PE matrix.

Measurement of *G*

The fracture toughness of the interface was measured with the asymmetric double-cantilever beam (ADCB) test because it is a reliable test for studying interface mechanisms on a molecular scale.[4–7] The efficiency of the connectors was evaluated in terms of the *G* value required to create an increment of a new surface as a razor blade was inserted at the interface. According to the Kaninnen model, eq. (1) can be used to calculate *G*:

$$G = \left(\frac{3E_1E_2h_1{}^3h_2{}^3\Delta^2}{8a^4}\right)\left[\frac{C_2{}^2E_1h_1{}^3 + C_1{}^2E_2h_2{}^3}{(C_2{}^3E_1h_1{}^3 + C_1{}^3E_2h_2{}^3)^2}\right] \quad (1)$$

where

$$C_1 = \left(1 + 0.64\frac{h_1}{a}\right)$$

$$C_2 = \left(1 + 0.64\frac{h_2}{a}\right)$$

The subscripts 1 and 2 refer to the top and bottom glass beams, *a* is the crack length (as shown in Fig. 1), *E* is Young's modulus of the glass, *h* is the thickness of the beam sections, and *D* is the opening displacement (which is assumed to be the thickness of the razor blade, 0.1 mm).

The set-up instrument was mounted on a Adamel Lhomargy DY25 tensile machine. A 0.1-mm-thick wedge cleaved the specimen at a low speed (3 μm/s) under the assumption that the measured energy release rate was equal to G_c, the critical energy release rate at zero velocity. The crack length ahead of the wedge was measured during a stable propagation step with a video camera.

Experimental techniques

The crystallization studies were carried out on pure polymers and on blends based on double-bond-terminated and pure PEs (50:50 w/w). The DSC experiments could not be carried out on corresponding silane-terminated PEs because they could condense to form dimers. It was assumed that the polymers used as precursors had the same behavior during crystallization that the functionalized ones had. The blends were prepared by the separate swelling of the polymers at 140°C in xylene, the mixing of the two polymers, and coprecipitation in methanol at room temperature. The blends were subsequently dried in vacuo at 100°C. Thermograms were recorded on a PerkinElmer DSC7 thermal analyzer under a nitrogen atmosphere. All the samples were considered after the following cycle: heating at 40°C min^{-1}, a stage at 150°C for 5 min, cooling at 10°C min^{-1}, a second stage at 50°C for 5 min, and a final heating to 200°C at 10°C/min. The theoretical melting enthalpy of a PE monocrystal was taken to be 280 J g^{-1} [15] to compute the crystallinity index (*X*) from the normalized area under the curve. This value needed to be considered only as a relative value (especially for the PE–hexene copolymer). The crystallization kinetic data were obtained from the exothermic peaks integrated with various crystallization times to determine the amount of transformation that had taken place.

WAXS measurements were carried out with a rotating-anode X-ray generator (Rigaku Ru200) operating at 200 mA and 40 kV with nickel-filtered Cu Kα radiation (λ = 1.45178 Å). Scans were performed with a Θ–2Θ geometry, and this ensured that 001 reflections were measured with optimal intensity. The polymer films were first removed from their glass supports, and parallel strips 2 or 5 mm were cut. The strips were piled up to form a 2-mm-thick stack, and the X-ray diagram of this stack was measured while the film surface was held perpendicular to the incident beam. For scans performed with the film surface parallel to the beam, one of the 5-mm-large strips was selected and held parallel to the beam. Additional scans were performed with a lead mask bearing a 0.3 × 3 mm^2 slit. This mask was positioned on the sample and slit parallel to the film surface, and the position was modified manually to illuminate the polymer section close to the glass interface, at the middle of the sample, or close to the matrix surface (Fig. 2).

Indexing was performed on the basis of the orthorhombic cell with an *a* axis of 7.417 Å, a *b* axis of 4.945 Å, and a *c* axis of 2.547 Å.[16] The half-widths (θ_B) were used to determine the crystallite size (*e*) in the corre-
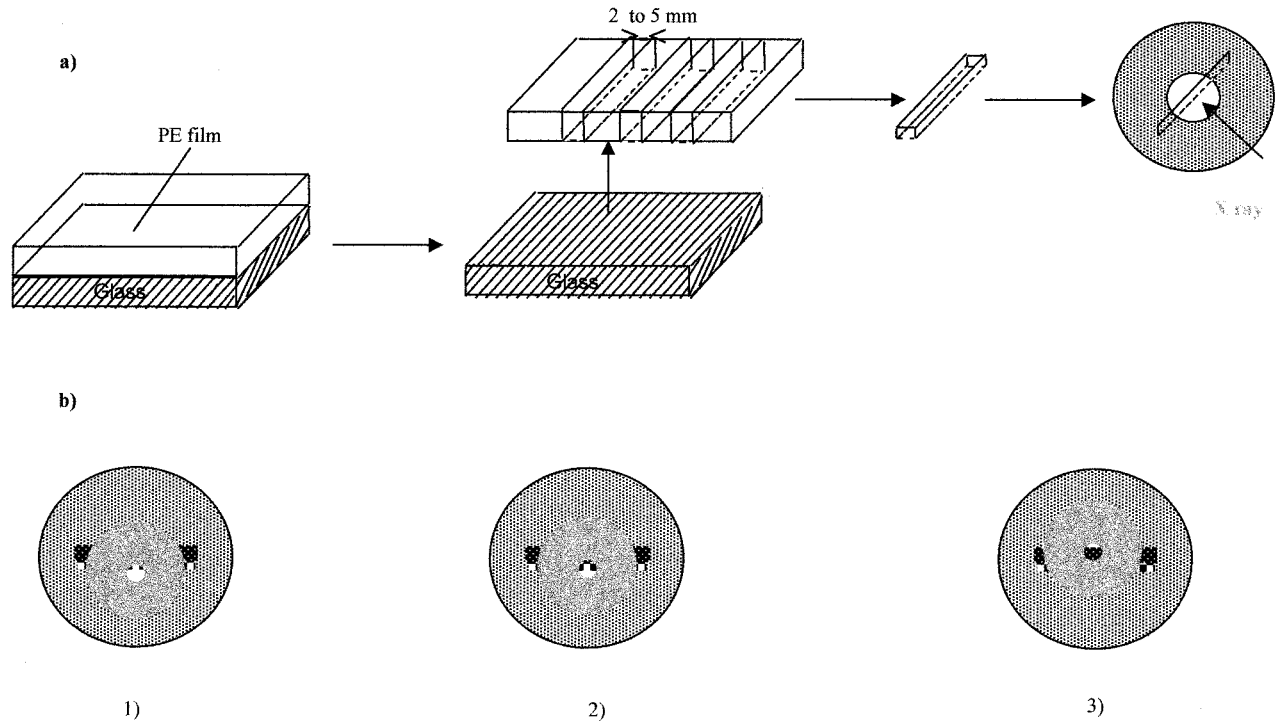
Figure 2 Specimen preparation for X-ray analysis: (a) the removal of the PE film from the glass support and the cutting of strips set on a lead support for analysis and (b) the position of the lead mask for analyzing a specific section [(1) close to the glass, (2) at the middle of the sample, and (3) close to the bulk PE matrix].

sponding directions from the Debye–Scherrer equation:

$$e_{hkl} \ (\text{Å}) = \frac{0.9\lambda \ (\text{Å})}{\theta_B \cos \theta_B}$$

RESULTS AND DISCUSSION

The addition of polymer chains as connectors at the glass/PE interface led to an increase in the fracture toughness of the interface. Large values of G were achieved, and a continuous increase was observed as the molar mass of the connecting chains increased (Fig. 3).
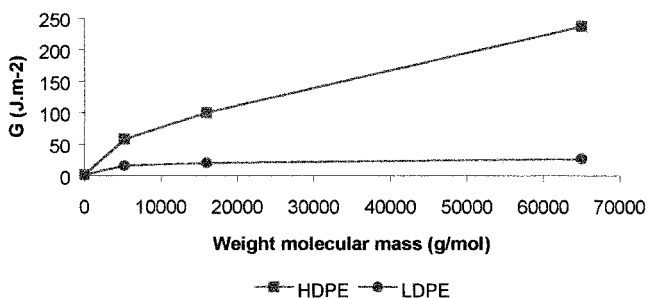

Figure 3 G for PE/glass interfaces as a function of the molar mass of the functionalized PE used as connecting chains.[13]

This effect could be related to the creation of entanglements between the tethered chains and free chains of the PE matrix. However, the interfaces prepared from the HDPE matrix displayed higher values of G than those based on the LDPE matrix (for the interfaces reinforced with the EH32500 copolymer, 240 and 30 J m^{-2}, respectively). In addition, the locus of the failure could be related to the nature of the PE matrix and the molar mass of the connecting chains. A cohesive failure in the bulk of the pure PE and the pullout of the grafted chains were the two mechanisms observed for the PE-grafted-glass/PE interfaces. The separated surfaces were examined with wettability measurements and atomic force microscopy. It was demonstrated that for the glass/LDPE reinforced interfaces, the grafted chains were extracted from the bulk PE, whereas for interfaces realized with the HDPE matrix, the failure occurred in the bulk of the matrix.[13] Therefore, it appears that the polymer connectors efficiently improved the coupling between the glass and HDPE matrix by forming an interphase with a cohesion stronger than that of the bulk one. From a mechanical point of view, it can be supposed that the structure of the interphase generated was different for the different types of matrices, that is, LDPE or HDPE. One hypothesis is that the linear structure of the HDPE chains can cocrystallize with the grafted ones.
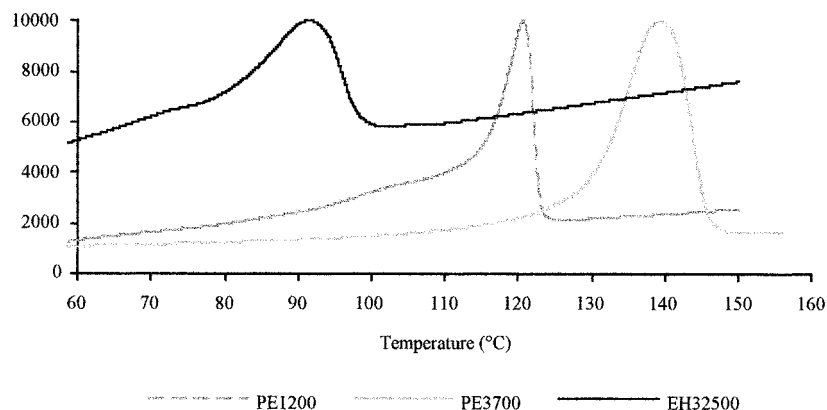
Figure 4 Melting endotherms for PE1200 and PE3700 and for copolymer EH32500 after cooling at 10°C min^{-1}.

The purpose of this work was to establish relationships between the fracture behavior of PE/grafted-glass interfaces and the crystalline morphology of the interphases.

Separate crystallizations of pure and functionalized PEs

Functionalized PE

The DSC endotherms of the double-bond-terminated PEs are shown in Figure 4. As expected for linear PEs such as PE1200 and 3700, T_m decreased as the molar mass decreased.[17] The shoulder that appeared for PE1200 on the low-temperature-side melting peak resulted from existing crystalline phases, as already reported by Paukkeri and Lehtinen,[18] who observed a double endotherm for the low molar mass PE. The observed shoulder on the melt endotherm of the copolymer was attributed to polyhexene.[12]

Table II reports the crystallization temperature (T_c), the enthalpies of melting (ΔH_f) and crystallization (ΔH_c), and crystallinity index (X) for the three functionalized polymers. The evolution of these parameters (T_c, T_m, and X) agrees with the polymer structure, that is, the molecular mass and tacticity. As expected, T_m increased with the molar masses of the homopolyethylenes. The hexene comonomer affected the chain regularity and implied steric hindrance in the chain. As a result, the hexene with its branched structure

hindered the crystallization, reducing X and T_m of copolymer EH32500.[19]

The WAXS spectra of the functionalized PE are reported in Figure 5. The spectra of two homopolyethylenes, PE1200 and PE3700, were quite similar to those reported in the literature.[20,21] This analysis allowed us to determine the crystallite dimensions from the relative intensity/diffraction angle plots. The three materials had sharp peaks at 21.5 and 24.5° corresponding to the (110) and (200) reflections, respectively. A broad peak could also be seen under these sharp peaks, with a maximum around 19.5°, corresponding to the amorphous halo. From an examination of the amorphous scattering peak located at about 19.5°, we can see that the peak was broader for the EH32500 copolymer, and this confirmed its lower crystallinity. X was also calculated from the ratio of the area under the crystalline peaks to the total area of the spectrum. X values calculated from DSC and WAXS were of the same order of magnitude but could differ according to the assumptions for each technique. In fact, it was assumed for WAXS that the amorphous phase in the semicrystalline polymer possessed the same structure as the totally amorphous melt (Table II). The dimensions of the crystallites were calculated from the (110) and (200) reflections and are reported in Table II. The (110) reflection corresponds to the diagonal in the a–b plane, whereas the (200) reflection corresponds to the direction perpendicular

TABLE II
Thermal (DSC) and WAXS Analyses of the Functionalized PE Connectors

Connectors	DSC				WAXS			
	T_c (°C)	T_f (°C)	ΔH_c (J g^{-1})	ΔH_f (J g^{-1})	X (%)	e_{110} (Å)	e_{200} (Å)	X (%)
PE1200	114	121	−149.4	138.3	49	493	681	44
PE3700	117	139	−197	192.1	69	313	434	50
EH32500	71	91.5	−40.6	48.2	17	69	a	19

a This value could not be taken into account because the resolution corresponding to the reflection [200] was not accurate enough in the case of copolymer EH32500.
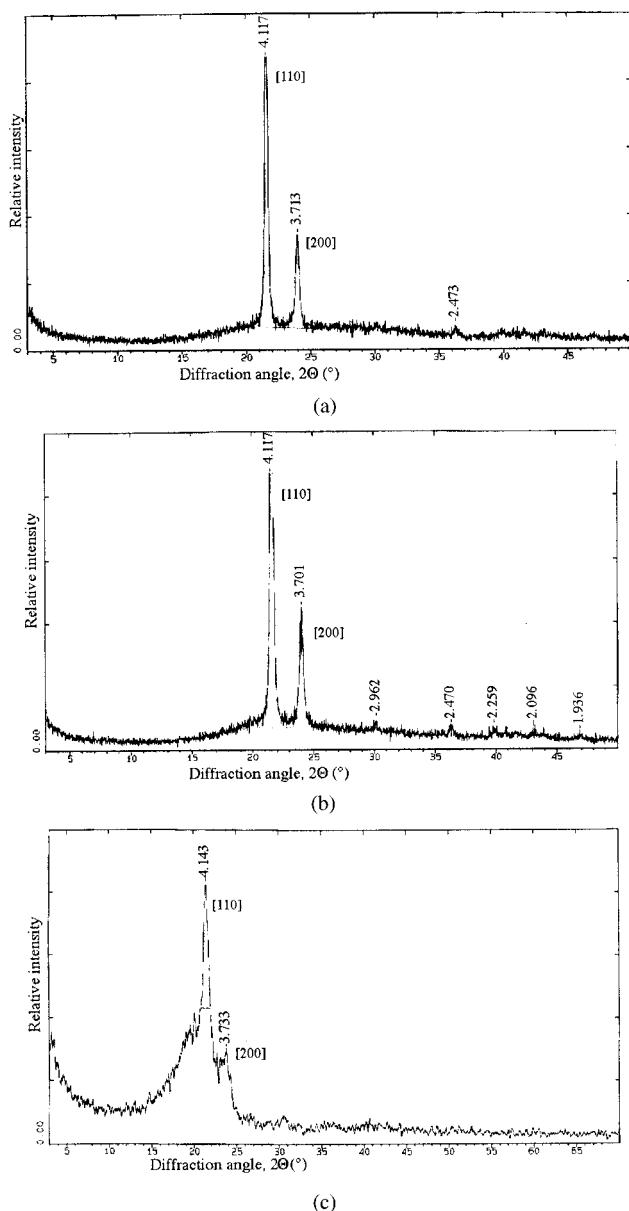
(a)

(b)

(c)

Figure 5 WAXD spectra of the functionalized PEs: (a) PE1200, (b) PE3700, and (c) EH32500.

to both the growth [(020)] and crystallites thickness [(002)] directions. As expected from DSC analysis, the homopolyethylenes showed thicker crystallites than the copolymers. As mentioned previously, the hexene comonomer hindered the crystallite growth. By comparing the thickness determined in both the (110) and (200) directions, we observed a preferential growth of crystallites in the direction perpendicular to the (200) plane.

Pure PEs (HDPE and LDPE)

The characteristic parameters of the DSC thermograms and the crystallite dimensions of the pure PEs

are given in Table III. As reported in the literature, the linear structure of HDPE led to a higher value of X and thicker crystallites than LDPE. In fact, the latter possessed short-chain branches that hindered crystallization. In both diffraction spectra (Fig. 6), the two main diffraction peaks of the crystalline phase of PE can be observed at 21.5 and 24°, corresponding to the (110) and (200) reflections, respectively.

Cocrystallization of the functionalized PE with pure PE

According to the literature, three main conditions are required for cocrystallization between polymers: (1) miscibility in the amorphous state, (2) similarity of crystalline forms, and (3) similarity of crystallization kinetics.

In this case, the components exhibited the same chemical and structural features, and this should favor miscibility. As demonstrated previously, WAXS analysis showed the same crystalline structure for both the functionalized PE and pure PE. The last requirement for cocrystallization between the PE connecting chains and the free PE chains, that is, evidence of similar crystallization kinetics, was studied by DSC for 50:50 (w/w) blends. The crystallization kinetics of the various components, reported in Figure 7, are indicative of the ability of the materials to cocrystallize.

In fact, the crystallization kinetics of the homopolyethylenes PE1200 and PE3700 and the HDPE matrix were quite similar, indicating that cocrystallization could occur. However, because of their branched structure, the LDPE matrix and the PE–hexene copolymer exhibited crystallization kinetics very different from the others'. As a result, cocrystallization between the copolymer and the HDPE free chains or between free LDPE and the grafted PE chains could not be obtained.

From the DSC analysis, the evidence for cocrystallization was based on the presence of a single melting peak and X. Figures 8 and 9 show the melting peaks of the blends based on functionalized PE and HDPE and LDPE matrices, respectively. For each, the endotherms of pure components are reported for comparison. The crystallization kinetics of the blends compared with those of the pure components are shown in Figures 10

TABLE III
Thermal (DSC) and WAXS Analyses of the Pure PE Matrices

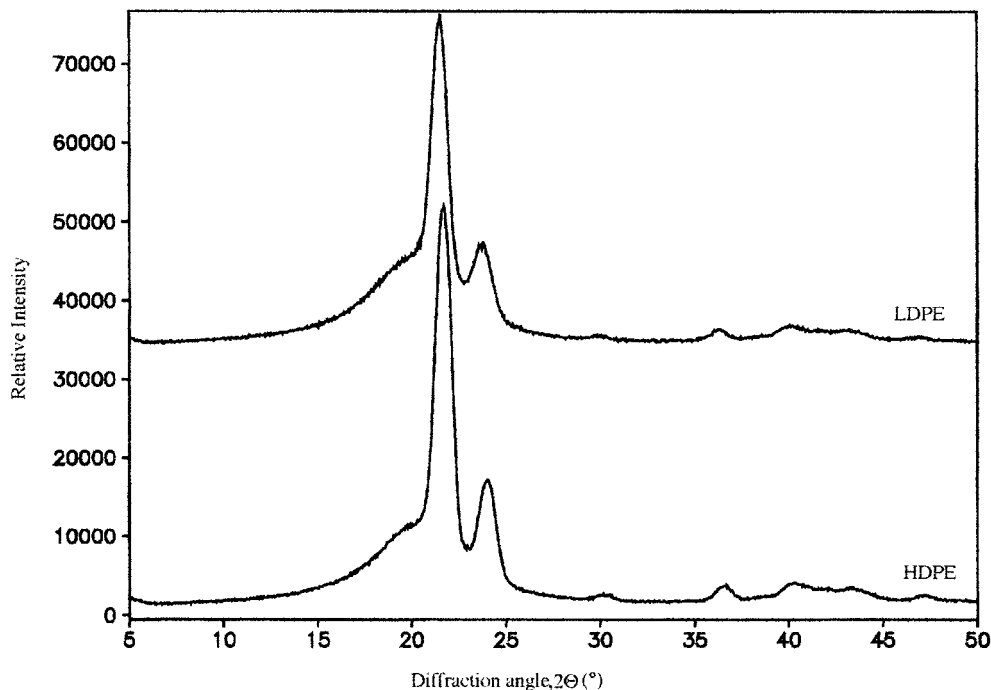| Pure PE	DSC				WAXS		
	T_c (°C)	T_m (°C)	ΔH_c (J g^{-1})	ΔH_f (J g^{-1})	X (%)	e_{110} (Å)	e_{200} (Å)
HDPE	115	126	−126	128	45.5	200	279
LDPE	95	112	−79	95	32	139	209

Figure 6 WAXD spectra of the pure PE matrices.

and 11 for HDPE- and LDPE-based blends, respectively, for both PE matrices.

The presence of a single melting peak for the HDPE/PE1200 blend was indicative of new crystallites formed by the free chains of the matrix and functionalized PE chains after quenching. Despite the similarity between the endotherms of the functionalized PE, PE1200, and the blend, the lack of a melting peak characteristic of the HDPE matrix on the DSC trace and the fact that the crystallization kinetics were similar [Fig. 10(a)] made clear the cocrystallization of the HDPE and PE1200. Moreover, X (58.3%) was

higher than that of the initial polymers crystallized under the same conditions (49.0 and 45.5% for PE1200 and HDPE, respectively).

For the HDPE/PE3700 blend, the presence of a melting peak at 117°C was also indicative of a new crystalline organization different from that of the pure components. This temperature was lower than that of the components, with a less perfect crystalline structure assumed. The crystallization kinetics for this blend, intermediate between the kinetics of the pure components [Fig. 10(b)], was associated with mixed crystalline lamellae, based on the chains of the two
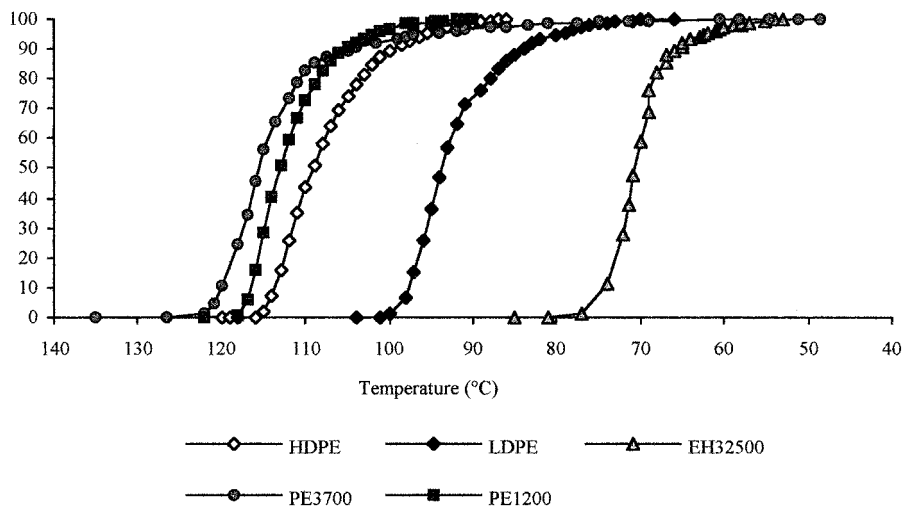

Figure 7 Crystallization kinetics determined by DSC analysis for the functionalized PE and the pure PE matrices (HDPE and LDPE).
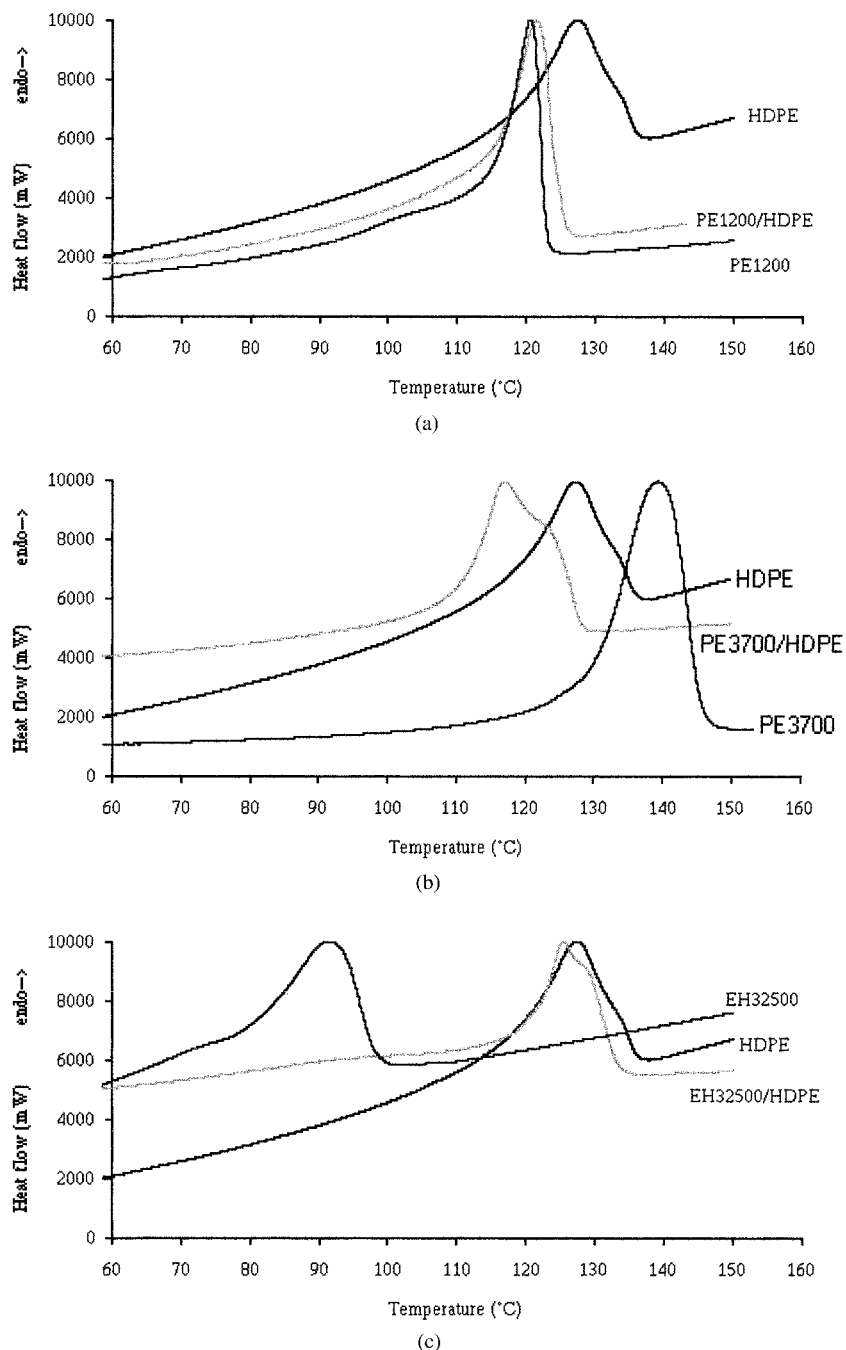
Figure 8 DSC traces of functionalized PE/HDPE blends (50:50 w/w) based on (a) PE1200, (b) PE3700, and (c) EH32500 as functionalized polymers (heating rate = 10 K min^{-1}).

components. Moreover, the 54% value of X observed was between the values of the initial components (45.5 and 68.5% for HDPE and PE3700, respectively). Overall, these observations showed that cocrystallization occurred for this system. However, the shoulder existing on the melting endotherm of the blend and associated with HDPE crystallites suggested that the cocrystallization was not complete.

As expected from the crystallization kinetics (Fig. 7), the melting thermogram of the blend based on HDPE

and EH32500 did not allow us to conclude that there was cocrystallization between these components. It was assumed that the copolymer microstructure prevented interdiffusion within the HDPE chains and, subsequently, cocrystallization. The single T_m on the DSC trace of the blend corresponded to that of the pure PE. This establishment was supported by the similarity of the crystallization kinetics of the blend and pure PE [Fig. 10(c)]. As the polymer chains of the HDPE matrix were able to crystallize, the copolymer
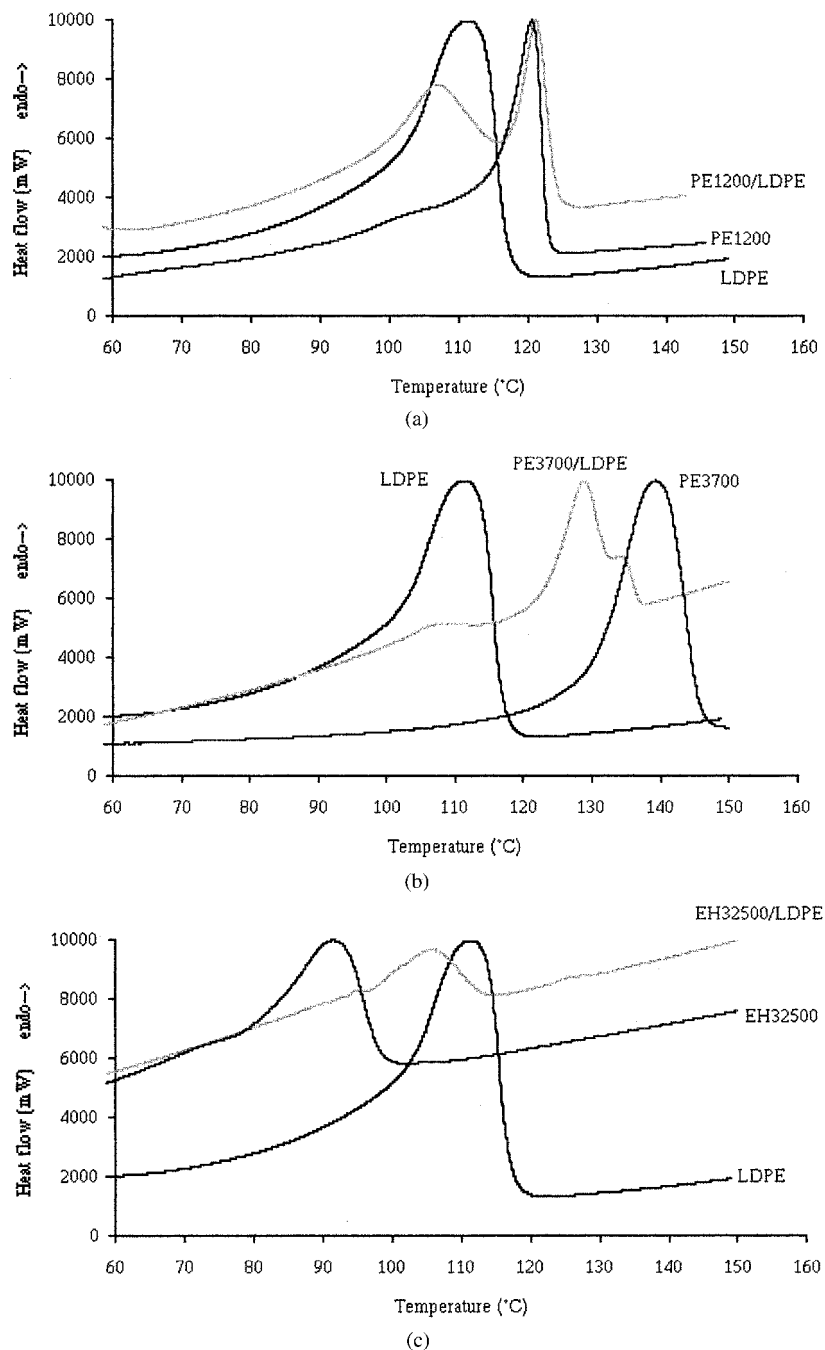
Figure 9 DSC traces of functionalized PE/LDPE blends (50:50 w/w) based on (a) PE1200, (b) PE3700, and (c) EH32500 as functionalized polymers (heating rate = 10 K min^{-1}).

chains were rejected in the amorphous parts. The rate of crystallinity ($X = 17\%$) of the pure copolymer was already low and became very low in the blend. In the crystallization thermogram of the blend [Fig. 12(a)], two exotherms can be made out. The first one, located at 110°C, was very close of that of the matrix ($T_c = $ 115°C for HDPE). The second one, with an intensity much lower and with a temperature domain of 70–90°C, was associated with the copolymer crystallites ($T_c = $ 71°C). The observed values of T_c were not sim-

ilar to those of the two pure polymers. A shift in the peaks, which seemed to be due to the mutual hindrance of the two polymers in the blend, was observed. The nonregular structure of the copolymer drastically reduced X of the HDPE matrix because X of the blend was only 16%, whereas X was 45.5% for the pure matrix crystallized under the same conditions.

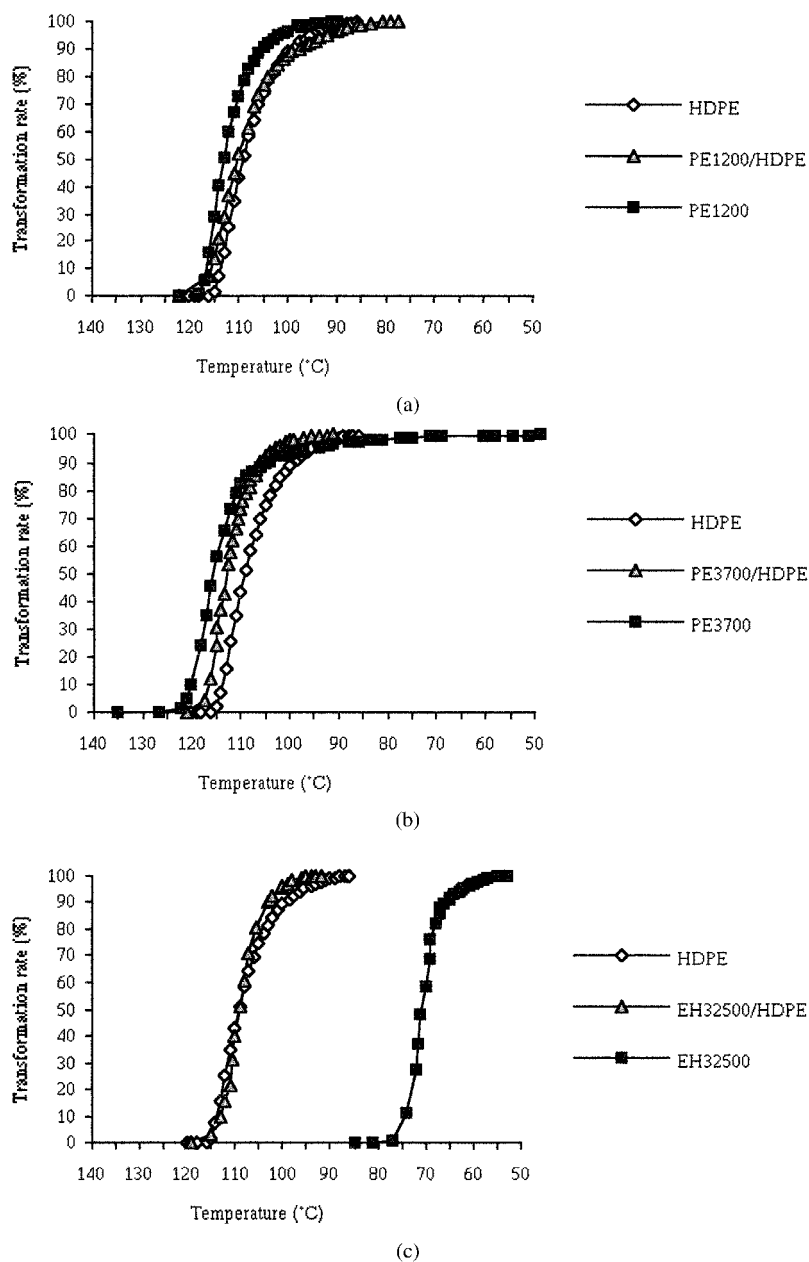Let us now consider the blends based on the LDPE matrix. For the blend based on PE1200 and LDPE in

Figure 10 Crystallization kinetics of blends based on functionalized PE and HDPE compared with those of the initial components. The blends were based on (a) PE1200, (b) PE3700, and (c) EH32500.

Figure 9(a), the thermogram exhibits two melting peaks that clearly show that there was no cocrystallization. Moreover, the crystallization DSC trace of this blend [Fig. 12(b)] displays two crystallization exotherms corresponding to the separate crystallizations of the pure components.

The behavior of the PE3700/LDPE blend was not so obvious. The melting peak was located at 129°C and could be attributed to a mixed crystalline structure. However, the high crystallinity of PE3700 ($X = 68.5\%$) suggested that this new structure could have come from the functionalized PE considered. This assumption was supported by the similarity of the crystalli-

zation kinetics of the blend and PE3700 [Fig. 11(b)]. Moreover, the crystallization exotherm of the blend ($T_c = 116°C$) seemed to correspond to that of PE3700 [$T_c = 117°C$; Fig. 12(c)], although there was a shift in T_m of the blend with respect to that of PE3700. This phenomenon could be due to the decreasing crystallites dimensions. The branched structure of the LDPE matrix hindered the crystallization of the PE3700 polymer, and as a result, X decreased (from 68.% to 29% for PE3700 and the blend, respectively). Furthermore, both shoulders observed on the blend endotherm, which obviously corresponded to the LDPE and PE3700 phases, respectively, were consistent with the
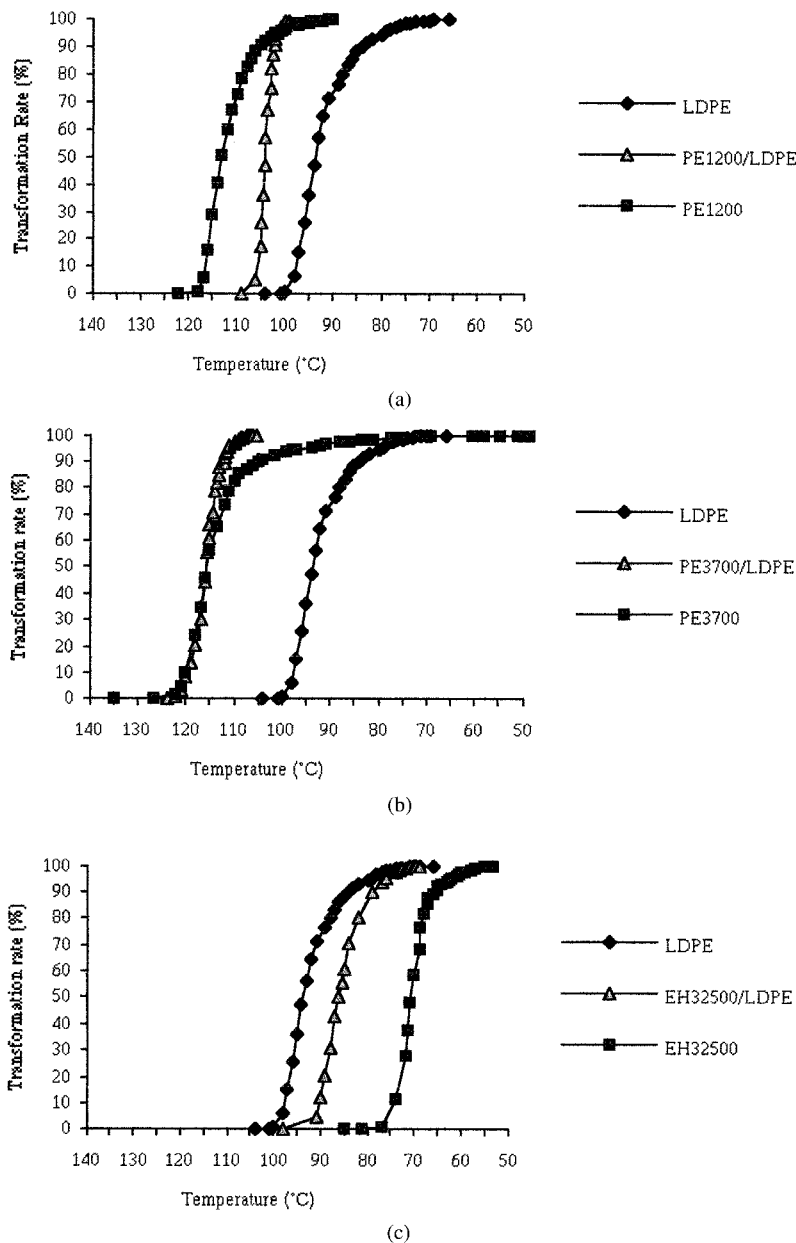
Figure 11 Crystallization kinetics of blends based on functionalized PE and LDPE compared with those of the initial components. The blends were based on (a) PE1200, (b) PE3700, and (c) EH32500.

presence of a phase with an intermediate density but not necessarily with a component resulting from cocrystallization.

The LDPE/EH32500 blend should have shown a low capacity for cocrystallization because both materials had nonregular structures. However, the blend exhibited a single endotherm and $T_f = T_m$ (107°C) and T_c (87°C) values intermediate to those of the two pure materials (Table II). Even if the presence of a single peak suggested possible cocrystallization, this one remained limited because of the nonregular structure of the copolymer, which hindered the crystallization of the blend ($X = 8\%$).

These DSC analyses showed that it was not easy to make firm conclusions concerning complete cocrystallization in the different blends. However, distinct trends could be seen in these measurements: (1) cocrystallization was observed between the HDPE matrix and modified polymers with a regular structure, that is, PE1200 and PE3700, and (2) the copolymer with hexene units seemed to be able to cocrystallize with the LDPE matrix even if the cocrystallinity index remained low because of the insertion of the hexene units in the PE chains.

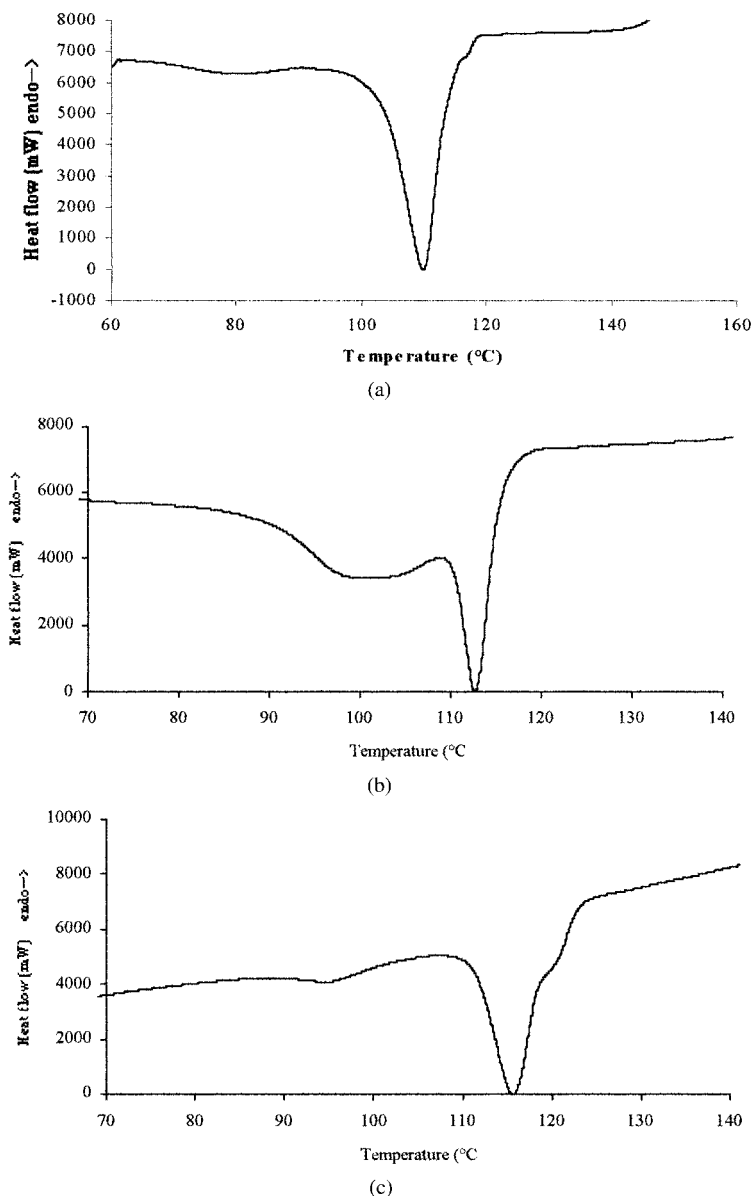However, the evidence for cocrystallization in blends of free chains was not representative of the

(a)

(b)

(c)

Figure 12 DSC traces recorded at a cooling rate of 10 K min^{-1} for functionalized PE/PE blends (50:50 w/w): (a) HDPE/EH32500, (b) LDPE/PE1200, and (c) LDPE/PE3700.

crystalline organization and mobility of chains grafted on surfaces. In fact, in such cases, the degree of mobility of the grafted chains is reduced, and as a result, their ability to crystallize will be affected.[12]

Crystalline organization at the interface

Another method for examining the interaction between the grafted PE chains and the free chains is X-ray diffraction. This method can provide information concerning the crystalline organization in the interphase by directly analyzing the film after fracture. Therefore, one may judge whether or not blends show a particular crystallinity at the angstrom level in the

vicinity of the interfacial region and if this represents a significant thickness in comparison with the total thickness of the detached film.

In both of the intensity–2Θ spectra of separated PE films reported in Figures 13 and 14, two main crystal-phase peaks at 21.5 and 24.5°, corresponding to the (110) and (200) reflections of PE, respectively, can be observed. Additional 2Θ peaks located at 31 and 36° corresponding to the (210) and (020) reflections appear with varying intensity, depending on the position of the film with respect to the X-ray beam. The four peaks are also present in the spectrum of the pure PE, although the latter two are much less intense. As a result, a preferential orientation was present that might have been the result of changes in the nucleating characteristics of the
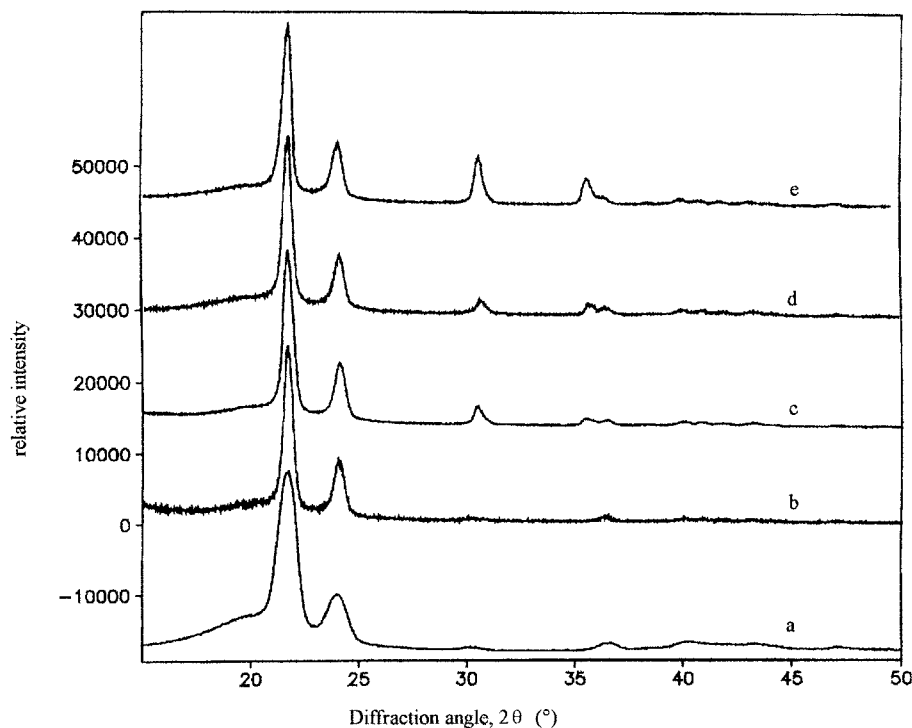
Figure 13 WAXD spectra of blends based on HDPE: (a) pure HDPE film (not detached from glass), (b) HDPE film after separation from ungrafted glass, (c) HDPE film after separation from EH32500-grafted glass, (d) HDPE film after separation from PE3700-grafted glass, and (e) HDPE film after separation from PE1200-grafted glass.

glass surface modified by grafted chains with different chain lengths and/or organization.[14] X-ray spectra were also recorded with a mask to observe the crystalline phase in the vicinity of the glass/PE interface (Fig. 15).

The intensity of the peaks decreased as the analyzed area moved away from the interface. This observation could be related unambiguously to the existence of an oriented interphase.
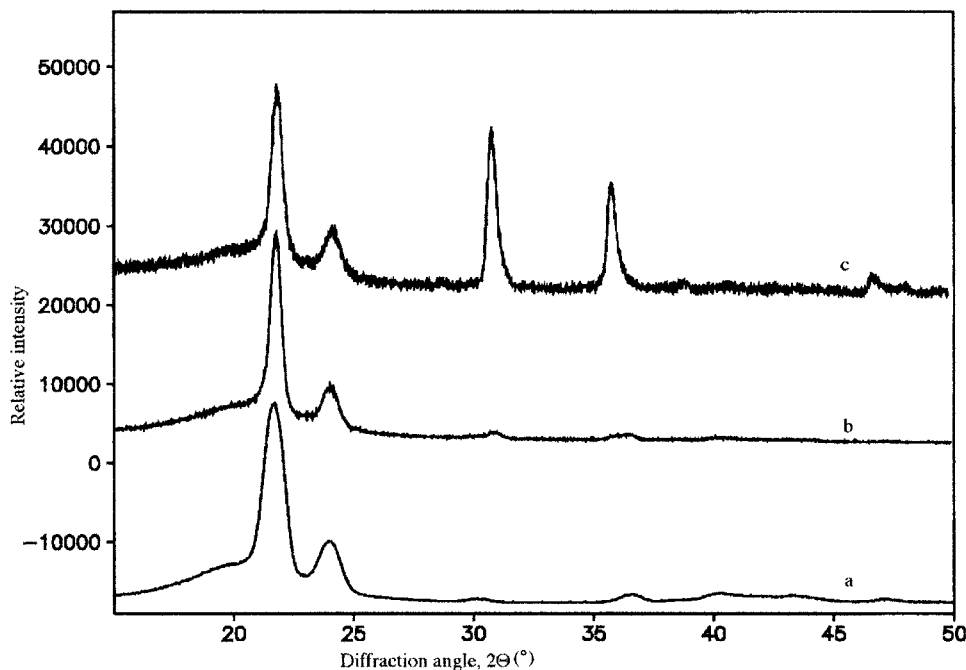

Figure 14 WAXD spectra of blends based on LDPE: (a) pure LDPE film (not detached from glass), (b) LDPE film after separation from PE3700-grafted glass, and (c) LDPE film after separation from EH32500-grafted glass.
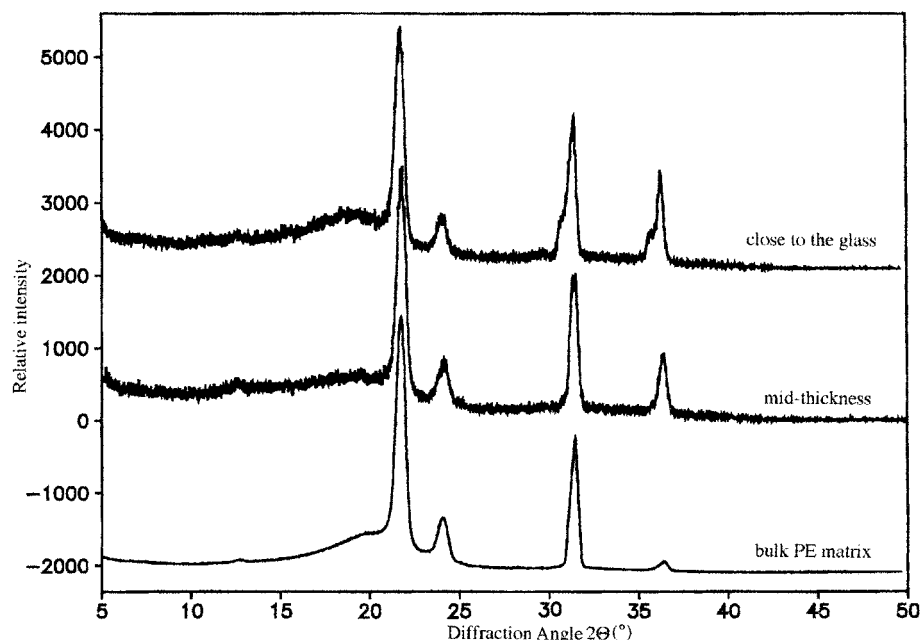
Figure 15 Changes in the WAXD spectrum shape as a function of the beam position in the PE3700/HDPE interphase.

In Figure 13, the spectra of detached HDPE films are given. These were recorded with an X-ray beam perpendicular to the surfaces of the films. In this position, the changes in the orientation were more easily detected from changes in the intensity ratio of the peaks. The (210) and (020) peaks had negligible intensity in the spectrum related to the film separated from an untreated glass surface. This shows that the orientation was not induced by the glass surface but was related to the presence of the PE-grafted chains. Therefore, these two additional diffraction peaks could be attributed to a specific crystalline orientation of chains at the interface. Furthermore, the relative intensity of these peaks related to the orientation in the vicinity of the grafted surface was dependent on the nature of the grafted chains. The orientation was more important because the connecting chains displayed a higher capacity for crystallization (i.e., shorter and linear chains).

For the interfaces resulting on LDPE films detached from glass (Fig. 14), the lack of intense 210 and 020 diffraction peaks indicated a low degree of orientation. This corresponded to the absence of a cocrystallization phenomenon, which was also concluded from the DSC analysis. However, as suspected from the DSC analysis, the X-ray spectrum of the EH32500/LDPE blend showed diffraction rays located at 31 and 36°. Because of the branched structures of both components, the chains were assumed to be slightly cocrystallized. Consequently, the X-ray results were surprising. Nevertheless, it must be remembered that the samples were observed after failure and that the

grafted chains of the copolymer were extracted from the bulk LDPE. According to the higher fracture energy of this type of interface, the wide-angle X-ray diffraction (WAXD) analysis characterized the orientation of the matrix after deformation, including large plastic deformation.

For the HDPE films, the highest orientation was observed for the PE1200/HDPE interface. In fact, such an orientation could be explained by the linear nature and short length of the connectors, which favored the cocrystallization phenomenon. Because the connector chain was grafted to the surface, cocrystallization occurred with a preferential orientation, inducing an orientation of chains at the interface. For the EH32500/LDPE interface, for which the strongest orientation was observed, the branched structures of both components favored chain interpenetration. As chains were pulled out, the deformation induced a strong orientation of the crystals in the deformed regions.

Moreover, this crystalline orientation varied in the interphase region. In fact, the (020) peak displayed a higher intensity as the analyzed area in the interphase was closer to the glass surface (Fig. 15). Finally, the comparison between the WAXD measurements realized on the samples parallel or perpendicular to the beam provided evidence for the crystalline orientation. This orientation was preferentially in the direction perpendicular to the beam as additional peaks were not present in the spectrum of the samples analyzed in a position parallel to the beam (Fig. 16).
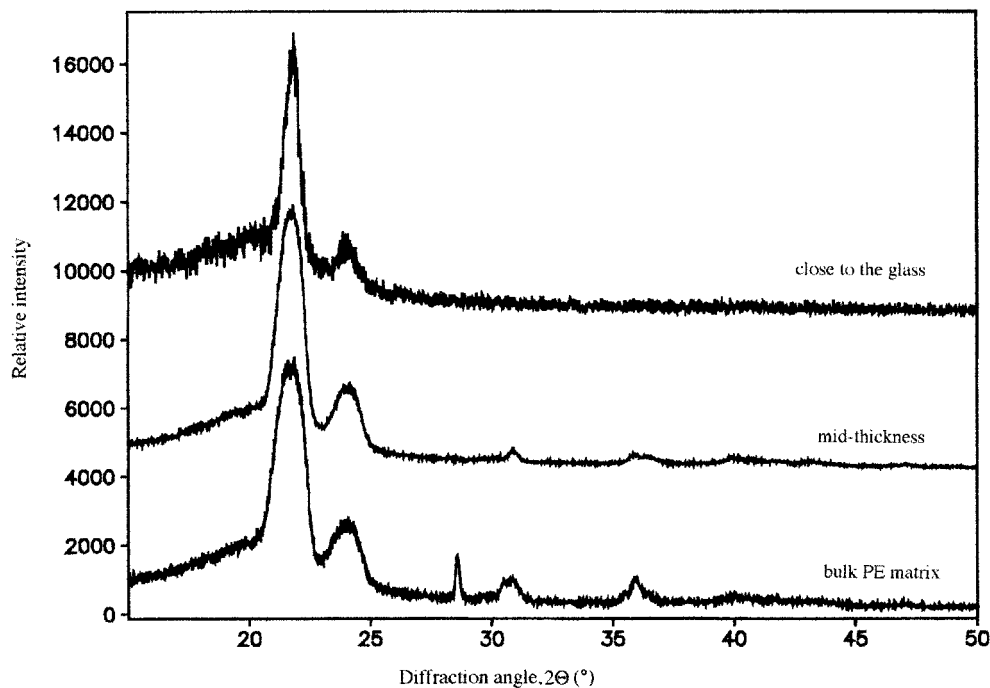
Figure 16 WAXD spectral intensity versus 2Θ for samples kept at a position parallel to the beam.

Relationships between the crystalline organization of the chains at the glass/PE interface and G

In a previous work,[13] it was demonstrated that the interfaces prepared from HDPE and grafted glass were so tough that the failure occurred in the bulk of the PE film. When the connectors displayed a linear structure (PE1200 and PE3700), a single DSC endotherm was observed for the blends, providing evidence that cocrystallization occurred. The WAXD spectra also showed a specific crystalline organization close to the interface. Therefore, the high toughness of such interfaces could be associated with cocrystallization in the vicinity of the glass surface. Nevertheless, G increased with the increasing molar mass of the connectors as the ability of the connector to cocrystallize with the PE free chains decreased; this demonstrated that the cocrystallization of grafted chains with the free chains (matrix) could not be the unique contribution to G. In fact, for the longest grafted chains (i.e., those of the copolymer displaying a low capacity for cocrystallization), an amorphous interphase was generated. In this case, the connectors could interdiffuse efficiently into the bulk of the PE film and form entanglements with the free chains so that a high fracture energy was reached (G_c = 240 J m^{-2}).[13]

The interfaces based on the LDPE matrix displayed lower values of G, and failure occurred from the pull-out of the grafted connecting chains.[13] No mixed crystalline organization at the linear PE (PE1200 or PE3700)/LDPE interface was evidenced. The linear chains had trouble with diffusing into the branched PE matrix, and so cocrystallization with the LDPE chains was limited. This limited interdiffusion led to weak adhesion (G_c < 20 J m^{-2}). The DSC and WAXD analyses showed that the grafted copolymer chains and free chains formed a mixed crystalline structure. However, this cocrystallization remained low (X = 8%) and was not sufficient to strengthen the interface (G_c = 27 J m^{-2}).

CONCLUSIONS

The crystallization phenomena occurring at the interface between PE-grafted glass and a PE matrix (HDPE or LDPE) were studied with DSC and WAXS experiments. The latter were performed on functionalized PE HDPE (or LDPE) blends and on PE films removed from grafted-glass surfaces (after ADCB tests). A specific crystalline orientation in the vicinity of the interface was evidenced for systems based on short grafted chains and linear free chains (i.e., HDPE), whereas for the longest grafted chains, which were not able to cocrystallize easily in blends and/or branched PE free chains, no specific orientation was evidenced at the interface. G was related to this crystalline organization in the vicinity of the glass surface. It was demonstrated that the crystalline nature of the interfacial regions could not be related directly to G. In fact, the highest value of G was obtained for the more amorphous interphase resulting from the interdiffusion of the longest grafted chains and the linear PE matrix (HDPE).

References

1. DiBenedetto, A. T. Compos Struct 1994, 27, 73.
2. Feller, J. F.; Guyot, A.; Spitz, R.; Chabert, B.; Gérard, J. F. Compos Interfaces 1995, 3, 121.
3. Creton, C.; Kramer, E. J.; Hadziioannou, G. Macromolecules 1991, 24, 1846.
4. Brown, H. R. Macromolecules 1989, 22, 2859.
5. Washiyama, J.; Creton, C.; Kramer, E. J. Macromolecules 1992, 25, 4751.
6. Brown, H. R.; Char, K.; Deline, V. R. Macromolecules 1993, 26, 4155.
7. Boucher, E.; Folkers, J. P.; Creton, C.; Hervet, H.; Leger, L. Macromolecules 1997, 29, 2102.
8. Boucher, E.; Folkers, J. P.; Hervet, H.; Leger, L.; Creton, C. Macromolecules 1996, 30, 774.
9. Lee, S. H.; Li, C. L.; Chung, T. C. Polymer 1994, 35, 2980.
10. Li, T.; Topolkaraev, A.; Hiltner, A.; Baer, E.; Ji, X. Z.; Quirk, R. P. J Polym Sci Part B: Polym Phys 1995, 33, 667.
11. Duvall, J.; Selliti, C.; Myers, C.; Hiltner, A.; Baer, A. J Appl Polym Sci 1994, 52, 207.
12. Feller, J. F. Ph.D. Thesis, Universite Lyon I, 1995.
13. Duchet, J.; Chapel, J. P.; Chabert, B.; Gérard, J. F. Macromolecules 1998, 31, 8264.
14. Duchet, J.; Chapel, J. P.; Chabert, B.; Spitz, R.; Gérard, J. F. J Appl Polym Sci 1997, 65, 2481.
15. Brandrup, J.; Immergut, E. H. Polymer Handbook; Interscience: New York, 1966.
16. Miller, R. L. In Crystalline Olefin Polymers; Raff, R. A. V.; Daak, K. W., Eds.; Wiley-Interscience: New York, 1965.
17. Encyclopedia of Polymer Science and Engineering, 2nd ed.; Beach, D. L.; Kissin, Y. V.; March, J.; Bikales, N. M.; Overberger, C. G.; Menges, G. J., Eds.; Wiley: New York, 1985; Vol. 6, p H61.
18. Paukkeri, R.; Lehtinen, A. Polymer 1993, 34, 4083.
19. Kissin, Y. V. Adv Polym Sci 1974, 15, 9.
20. Minick, J.; Moet, A.; Baer, E. Polymer 1995, 36, 1923.
21. Kalendo, M.; Ullmann, R. J Polym Sci 1960, 45.